ECI 8th International Conference on Boiling and Condensation Heat Transfer
Ecole Polytechnique Fédérale de Lausanne, 3-7 June 2012
Lausanne, Switzerland

THEORETICAL MODELING OF THE CONDENSATION PHENOMENA IN THE DEHUMIDIFIER OF THE SEAWATER GREENHOUSE

T. Tahri1*; M. Amoura2; S.A. Abdul-Wahab3; A. Bettahar4 and M. Douani5
Department of Electrical Engineering
University of Hassiba Ben Bouali
Chlef, 02000, Algeria
E-mail: t.tahri@univ-chlef.dz

ABSTRACT

The objective of this study is to develop theoretical models to describe the physical processes of condensation of humid air in the dehumidifier of the seawater greenhouse. The developed models were based on the heat and mass balances according to the thermodynamic model of Nusselt. The models were applied to the dehumidifier of the seawater greenhouse that is located at Al Hail in Muscat, Oman. The saturation temperature of humid air and the heat transfer coefficient of condensation were calculated for each tube along the length of the dehumidifier. The simulated condensate values were compared with that of the actual measured values. The relationships between the amount of condensate and other variables such as the relative humidity, the air dry bulb temperature, the seawater temperature, the humid air flow, the seawater flow and the solar radiation were investigated.

INTRODUCTION

The seawater greenhouse (SWGH) process makes use of sunlight, seawater and the ambient air to produce freshwater and colder air, creating more temperate conditions for the cultivation of crops at remote and arid coastal areas. The Seawater Greenhouse desalination by humidification–dehumidification uses a tubular condenser with external condensation. Seawater circulates inside the tubes while vapour condenses on the external walls of the tubes. The bottleneck of the greenhouse desalination by humidification and dehumidification (SWGH) is the design of condenser. Mahmoudi et al (2010) shows that for a given cooling water temperature, the rate of condensation increase with increasing length of the tube. An economic study by Goosen et al (2011) can define a compromise between the length of the tube to be used and the necessary temperature of the cooling water. Thermodynamic modeling of the Seawater Greenhouse system has shown that the dimension of the greenhouse (i.e. width to length ratio) had the greatest overall effect on water production and energy consumption. According to Davies et al (2005), the optimum airflow for water production is of the order 5 m^3/s. For cooling, a flow of 10–20 m^3/s appears more appropriate. In reality this can be overcome partially by maintaining a large flow through the greenhouse while allowing some air to bypass the water production stages of the second evaporator and condenser. Paton and Davies (2006) shows that if we wish to have a more uniform temperature profile across the length of the greenhouse, it should either be made shorter, or the air flow rate increased. Perret et al (2005) shows that the condenser was cold enough to condensate air moisture, the high airflow velocity limits the time required to maximize the number of water molecules at the vapour phase which are brought below dew-point. In other words, air speed did not allow sufficient time for surface contact between the moist air and the condenser to reduce air temperature below saturation. Air velocity regulation through the condensers by varying the fans speed with a frequency converter should be investigated to optimize condensation through the condenser. Dawood et al (2006) shows that, the freshwater production rate decreases as the ambient air relative humidity increases for each ambient air dry-bulb temperature. As the state of air entering the condenser is fixed, the amount of condensate depends mainly on the temperature of the condenser coolant. According to Davies et al (2004), a lower relative humidity results in a lower wet-bulb temperature. This means that colder water is fed into the condenser. Meanwhile, the air is also entering the Greenhouse at a cooler temperature. This favours the absorption of heat through the walls of the Greenhouse. Further, it is possible to choose a slightly lower ventilation rate without encountering overheating in the greenhouse. Consequently, a larger temperature differential tends to occur at the condenser which favours heat transfer and fresh water output.

The aim of this study is the simulation of the condensation in the condenser using heat and mass models. The influence of the operating parameters on fresh water produced by the condenser of seawater greenhouse was also investigated.

CONDENSER PROCESS DESCRIPTION

The condenser of the seawater greenhouse is described by Tahri et al (2009). It is a heat exchanger where the seawater is the coolant and the humid air is the hot fluid. The condenser consists of a set of 302 rows of parallel tubes arranged vertically and

with an angle of 30 degrees with the direction of flow of humid air. Each row has 14 identical vertical tubes with diameter of 33 mm (D) and a height of 1.8 m (L). Values of different design parameters of the condenser unit are listed in Table 1. The arrangement of the tubes was organized to ensure the passage of coolant from one tube to another. All tubes passes in a single row have the form of a coil. Seawater enters with a constant speed (u_{sw}) and a known temperature (T_{swin}) in the first row of each tube and it leaves the last tube in the same row with a temperature T_{swout}. The humid air from the second evaporator runs perpendicular to the condenser. It enters through the tubes with a velocity (v_{air}), temperature (T_{dbin}), and a relative humidity (RH_{in}). This humid air will leave the condenser with the same speed (v_{air}), with a temperature of T_{dbout} and a relative humidity of RH_{out}. The contact of humid air with the outer cold surfaces of the tubes of the condenser (in which seawater is flowing) will result in the condensation of the water vapor at the outer surfaces of these tubes (Figure 1). The produced condensate which will be formed as a liquid film of low thickness will descend along the tubes to be collected in the reservoir of fresh water.

Table 1
Design parameters of the condenser unit.

Dimensions of condenser	(15 ×1.9 × 0.8)m
Thickness of vertical tube (δ)	200 µm
Height of vertical tube (L)	1.8 m
Diameter of vertical tube (D_{out})	33 mm
Number of longitudinal tubes (N_L)	16
Number of transverse tubes (N_T)	302
Total number of tubes (N_{tot})	4832

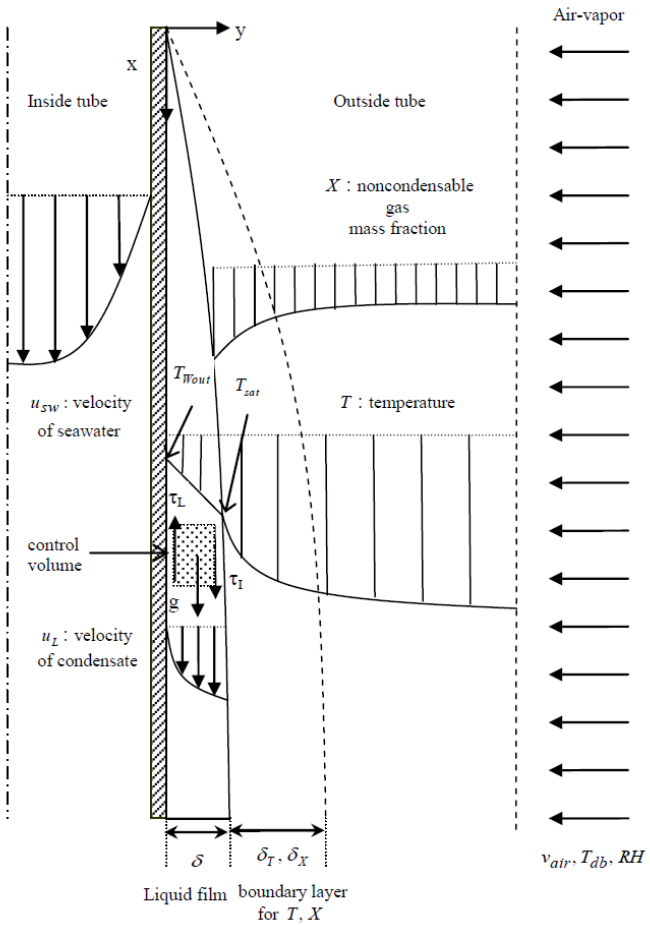

Figure 1 Process schematic of one vertical tube of the condenser unit.

MODELING OF HEAT AND MASS EXCHANGE IN THE CONDENSER

Steam condensation occurs when its temperature is reduced below its saturation temperature at a given pressure. Maheshwari et al (2004) shows that, the presence of non-condensable gases (air) in the gas mixture leads to a significant reduction in heat flow and during condensation because the non-condensable gases bind to the wall film preventing the diffusion of vapor through the bulk liquid film. Analysis of the kinetics of heat transfer for film condensation outside vertical tubes was originally treated for laminar film by Nusselt (1916). Our simulation of the condenser of the seawater greenhouse at Al-Hail,

Muscat, is based on a model developed previously by Douani et al (2011). Data of dry bulb temperature of air together with its relative humidity are collected only at the inlet and the exit of the condenser of the seawater greenhouse. Simulation of the operation of the condenser requires that the saturation temperature to be known at each tube of the condenser. Information about equations used can be found in Sherwood and Comings (1932).

Saturation temperature (T_{sat}) was calculated for the first and the last tube in the row of the condenser according to Eq. (1):

$$\frac{H_{sat}-H}{T_{sat}-T_{db}}=-\frac{C_s}{h_{fg}} \tag{1}$$

C_s is the mass humid heat (kJ/kg °C) which was calculated according to Eq. (2):

$$C_s = C_{pair} + H\, C_{pvap} \tag{2}$$

The temperature of seawater flowing inside the tubes of the condenser is only known at the entrance and exit of the condenser. In this work, parabolic interpolations were used to find the temperature of seawater at the entrance and the exit for each tube of the condenser by utilizing the information known at the entrance and exit of the condenser. As a basis of calculation, the temperature of seawater at the entrance and the exit of intermediate tubes are unknown. To resolve this problem, we opted for a linear profile of seawater temperature along the row of the condenser. The temperature at the entrance of each tube was calculated according to Eq. (3):

$$T_{swin}(j)=\left(\frac{(T_{swout}(16)-T_{swin}(1))}{16}\right)(j-1)+T_{swin}(1) \tag{3}$$

However, this hypothesis was subsequently corrected by introducing a coefficient of weighting that was used to adjust the value of the entrance seawater temperature for each tube. If the total number of tubes in the condenser N_{tot}, then the total flow of condensate will be:

$$\dot{m}_{ctot}=\sum_{j=1}^{N_L}\sum_{i=1}^{N_T}\dot{m}_{ij} \tag{4}$$

In addition, it was considered that the outlet seawater temperature T_{swout} of one tube of the row is equal to the inlet seawater temperature (T_{swin}) of the next tube. Also, it was assumed known both the inner (T_{Win}) and the outer wall (T_{Wout}) temperatures for the first tube in the row of condenser.

HEAT TRANSFER MODEL

This section presents the procedure of calculating the average heat transfer coefficient for film condensation **(** h_{ave} **)** for laminar film condensation on the outer surfaces of vertical tubes (i.e., liquid film is assumed to be laminar for the film thickness calculation). Figure 1 shows the physical model for film condensation on a vertical tube considered in Nusselt's analysis. The outer wall temperature is below the saturation temperature ($T_{Wout} \langle T_{sat}$) and thus the water vapor condenses on the outer surface of the tube. The liquid film flows downward under the influence of gravity. According to Çengel (2003), the film thickness and thus the mass flow rate of the condensate increases with x as a result of continued condensation on the existing film. Then the heat transfer from the vapor to the tube must occur through the film, which offers resistance to heat transfer. Clearly the thicker the film, the larger its thermal resistance and thus the lower the rate of heat transfer.

For the liquid film, the force balance in the control volume (Figure 1) can be expressed as

$$\tau_L = (\rho_L - \rho)\, g\, (\delta - y) + \tau_I \tag{5}$$

According to Seungmin et al. [14], the velocity profile in the liquid laminar film (u_L) can be described from the Eq. (5):

$$u_L(y)=\frac{(\rho_L-\rho)\, g}{\mu_L}\left(\delta\, y-\frac{y^2}{2}\right)+\frac{\tau_I}{\mu_L}y \tag{6}$$

The first term in the right hand side of Eq. (6) is the parabolic velocity distribution, which is exactly same with Nusselt analysis for no interfacial shear. The second term is the linear velocity distribution due to the interfacial shear. The liquid film mass flow rate ($\dot{m}_c$) can be calculated by integrating the velocity profile equation. Then, mass balance in liquid film can be expressed with respect to film thickness as indicated in Eq. (7):

$$\Gamma \equiv \frac{\dot{m}_c}{\pi\, D_{out}}=\left[\frac{(\rho_L-\rho)\, g}{3\,\nu_L}\,\delta^3+\frac{\tau_I}{2\,\nu_L}\,\delta^2\right] \tag{7}$$

From Eq. (7), the film thickness can be calculated. If there is no interfacial shear, the Nusselt thickness $\delta(x)$ can be explicitly defined as

$$\delta(x) = \left[\frac{4\, k_L\, \mu_L\, (T_{sat} - T_{Wout})\, x}{g\, \rho_L\, (\rho_L - \rho_v)\, h_{fg}} \right]^{\frac{1}{4}} \quad (8)$$

For laminar film, the temperature distribution in the film region is almost linear. Therefore the heat transfer coefficient for film condensation (h_x) at location x can be written as Eq. (9)

$$h_x = \frac{k_L}{\delta(x)} \quad (9)$$

Substituting the $\delta(x)$ expression from Eq. (8) into Eq. (9), the local heat transfer coefficient for film condensation h_x can be expressed as

$$h_x = \left[\frac{g\, \rho_L\, (\rho_L - \rho_v)\, h_{fg}\, k_L^3}{4\, \mu_L\, (T_{sat} - T_{Wout})\, x} \right]^{\frac{1}{4}} \quad (10)$$

However, the condensate in actual condensation process is cooled further to some average temperature between T_{sat} and T_{Wout}, releasing more heat in the process. Therefore, the actual heat transfer will be larger. According to ÇENGEL (2003), Rohsenow (1952) showed that the cooling of the liquid below the saturation temperature can be accounted for by replacing h_{fg} by the modified latent heat of vaporization h_{fg}^*, defined as

$$h_{fg}^* = h_{fg} + 0.68\, C_{pL}\, (T_{sat} - T_{Wout}) \quad (11)$$

The average heat transfer coefficient for laminar film condensation over the vertical tube of height L is determined from its definition by substituting the h_x relation and performing the integration. It gives:

$$h_{ave} = 0.943 \left[\frac{g\, \rho_L\, (\rho_L - \rho_v)\, k_L^3\, h_{fg}^*}{\mu_L\, (T_{sat} - T_{Wout})\, L} \right]^{\frac{1}{4}} \quad (12)$$

In the presence of noncondensble gases (e.g., air), the average heat transfer coefficient for film condensation (h_{ave}) was corrected (h_{vert}) according to the graph of Sacadura (1982) as shown in Eq. (13). The correction is a function of the noncondensable gas mass fraction (X)

$$h_{vert} = h_{ave}\, f(X) \quad (13)$$

X is the noncondensable gas mass fraction (kg noncondensable gas /kg total air) which was calculated for each tube according to Eq. (14):

$$X = \frac{m_{NC}}{m_{tot}} = \frac{1}{1 + H} \quad (14)$$

The heat flux (Q) in the film condensation was calculated for the first tube according to Eq. (15):

$$Q = h_{vert}\, A_{out} (T_{sat} - T_{Wout}) \quad (15)$$

The inner heat transfer coefficient h_{in} was calculated according to Eq. (16):

$$h_{in} = \frac{Nu\, k_{sw}}{D_{in}} \quad (16)$$

The outer wall temperature $(T_{Wout})_{cal}$ was then calculated for the first tube according to Eq. (17):

$$Q = 2\, \pi\, L\, k_{tub} \frac{\left((T_{Wout})_{cal} - (T_{Win}) \right)}{\ln\left(\frac{D_{out}}{D_{in}} \right)} \quad (17)$$

The inner wall temperature $(T_{Win})_{cal}$ was then calculated for the first tube according to Eq. (18):

$$Q = h_{in}\, A_{in} \frac{\left((T_{Win})_{cal} - T_{swin} \right) - \left((T_{Win})_{cal} - T_{swout} \right)}{\ln\left(\frac{\left((T_{Win})_{cal} - T_{swin} \right)}{\left((T_{Win})_{cal} - T_{swout} \right)} \right)} \quad (18)$$

The calculated $(T_{Wout})_{cal}$ from Eq. (17) and $(T_{Win})_{cal}$ calculated from Eq. (18) were then compared with the assumed values of T_{Wout} (Eq. 12) and T_{Win} (Eq. 17). If the compared values were different, the values of $(T_{Wout})_{cal}$ and $(T_{Win})_{cal}$ were

used in Eqs. (12) and (17) and the rest of the equations and then new values of $(T_{Wout})_{cal}$ and $(T_{Win})_{cal}$ are computed from Eqs. (17) and (18). The process is repeated until the values of $(T_{Wout})_{cal}$ and $(T_{Win})_{cal}$ with successive trials do not change.

The mass flux of condensate for the first tube can be determined by Eq. (19):

$$\dot{m}_{c1} = \frac{h_{vert}\ A_{out}\ (T_{sat} - T_{Wout})}{h_{fg}^{*}} \tag{19}$$

The heat flux transferred from humid air to seawater (Q_{sw}) was calculated in the first tube according to Eq. (20):

$$Q_{sw} = \rho_{sw}\ u_{sw}\ C_{Psw}\ \pi\ \frac{(D_{in})^2}{4}(T_{swout} - T_{swin}) \tag{20}$$

The enthalpy of air (H_{air}) was calculated at the entrance of the first tube according to Eq. (21):

$$(H_{air})_{in} = C_{Pair}\ T_{db} + H(C_{Pvap}\ T_{db} + h_{fg}^{0}) \tag{21}$$

The heat flux of air (Q_{air}) was calculated at the entrance of the first tube according to Eq. (22):

$$(Q_{air})_{in} = (H_{air})_{in}\ \dot{m}_{air} \tag{22}$$

The heat flux of air (Q_{air}) was calculated at the outlet of the first tube according to Eq. (23):

$$(Q_{air})_{out} = (Q_{air})_{in} - Q - Q_{sw} \tag{23}$$

The humidity of air (H) at the dry bulb temperature was calculated at the outlet of the first tube according to Eq. (24):

$$H_{out} = H_{in} - (\frac{\dot{m}_{c1}}{\dot{m}_{air}}) \tag{24}$$

The dry bulb temperature T_{db} was calculated at the outlet of the first tube according to Eq. (25):

$$T_{dbout} = \frac{\frac{(Q_{air})_{out}}{\dot{m}_{air}} - (H_{out}\ h_{fg}^{0})}{C_{Pair} + (H_{out}\ C_{Pvap})} \tag{25}$$

The calculated humidity of air $(H_{out})_{cal}$ from Eq. (24) and dry bulb temperature $(T_{dbout})_{cal}$ from Eq. (25) in outlet first tube were used in Eq. (1) to set the saturation temperature (T_{sat}) of the second tube in the row of the condenser. Simulation of the condenser operation required that the saturation temperature to be known at each tube in the condenser. For this purpose, Eqs. (1-25) were repeated for each tube. Next, the total mass flow calculated $(\dot{m}_{c1tot})_{cal}$ from Eq. (4) was compared with the measured total mass flow $(\dot{m}_{ctot})_{m}$. According to Douani et al (2011), if the model was not valid, then new values were proposed for the coefficients of weighting of parabolic interpolation for seawater temperature at different tubes in the condenser. The trial was repeated until the values of $(\dot{m}_{c1tot})_{cal}$ and $(\dot{m}_{ctot})_{m}$ did not change with successive trials.

Mass transfer model

For this model, Eqs. (1-18) were repeated for the first tube to defined (T_{sat}) and (T_{Wout}).

The Reynolds analogy is very useful relation, and it is certainly desirable to extend it to a wider range of Pr and *Sc* number. Several attempts were done in this regards, but the simplest and the best know was the one suggested by Chilton and Colburn in 1934 as:

$$\frac{f}{2} = St\ \mathrm{Pr}^{2/3} = St_{mass} Sc^{2/3} \tag{26}$$

For $0.6 < Pr > 60$ and $0.6 < Sc > 3000$. This equation is known as the Chilton-Colburn analogy. Using the definition of heat and mass Stanton numbers, the analogy between heat and mass transfer was expressed more conveniently as:

$$\frac{h_{vert}}{h_{mass}} = \rho_{air} C_{pair} \left(\frac{Sc}{\mathrm{Pr}}\right)^{2/3} \tag{27}$$

For air-vapor mixtures at 298 K, the mass and thermal diffusivities were D = 2.5 10^{-5} m^2/s and α =2.18 10^{-5} m^2/s, respectively. Hence, Lewis number was calculated from Eq (28):

$$Le = \frac{\alpha}{D} = 0.872 \tag{28}$$

Next, $(\alpha /D)^{2/3} = 0.872^{2/3}$ was calculated as 0.913, where the value was close to unity. The Lewis number was relatively insensitive to variations in temperature. Therefore, for air-water vapor mixture, the relation between heat and mass transfer coefficients was expressed with a good accuracy as:

$$h_{mass} \cong \frac{h_{vert}}{\rho_{air} C_{pair}} \tag{29}$$

where ρ_{air} and C_{pair} are the density and specific heat of air at film temperature. The film temperature (T_{film}) was calculated according to Eq. (30):

$$T_{film} = \frac{T_{db} + T_{Wout}}{2} \tag{30}$$

The condensate rate of fresh water produced for the first tube was calculated by the following relation:

$$\dot{m}_{c2} = h_{mass} \pi D_{out} L \left(\rho_{vapdb} - \rho_{vapWout}\right) \tag{31}$$

where ρ_{vapdb} and $\rho_{vapWout}$ are the density of vapor at dry bulb and external wall temperature which were calculated according to Eq. (32):

$$\rho_{sat}(T) = \frac{2910 \exp(9.48654 - 3892.7/(T - 42.6776))}{8314\, T} \tag{32}$$

Simulation of the condenser operation requires that the saturation temperature to be known at each tube in the condenser. To this end, Eqs. (20-25) were repeated for each tube. Next, the total mass flow calculated $(\dot{m}_{c2tot})_{cal}$ from Eq. (4) was compared with the measured total mass flow $(\dot{m}_{ctot})_m$. If the model was not valid, then new values were proposed for the coefficients of weighting of parabolic interpolation for seawater temperature at different tubes in the condenser. The trial was repeated until the values of $(\dot{m}_{c2tot})_{cal}$ and $(\dot{m}_{ctot})_m$ did not change with successive trials.

SIMULATION OF OPERATIONAL PARAMETERS OF CONDENSER

The mass model developed in this work reflects very closely the dynamic behavior of the condenser of the greenhouse. It is quite obvious that the optimal performance cannot be achieved if only the analysis of the influence of parameters is studied. So, the next part will be dedicated to the study of actual conditions of operation of the greenhouse. To this end, the authors defined the range of variation of different parameters. Thus, it has been noted the following:

- Relative humidity of inlet air dry (RH_{in}) varies from 0.8 to 0.98%.
- The inlet temperature of humid air (T_{dbin}) varies from 30 to 50 °C.
- The temperature of the seawater at the entrance (T_{swin}) varies from 20 to 30 °C.
- The mass flow of humid air input ($\dot{m}_{air}$) varies from 11.74 to 23.48 kg/s.
- The mass flow of entry of sea water ($\dot{m}_{sw}$) varies from 3.81 to 14.52 kg/s.

RESULTS AND DISCUSSIONS

Figure 2 illustrate the calculated and measured mass condensate rates. It was observed that the trend of the predicted and the measured mass condensate rates were close. The trend of the predicted mass condensate rates calculated in this work by mass model was much closer to the measured condensate rates than that calculated by heat model.

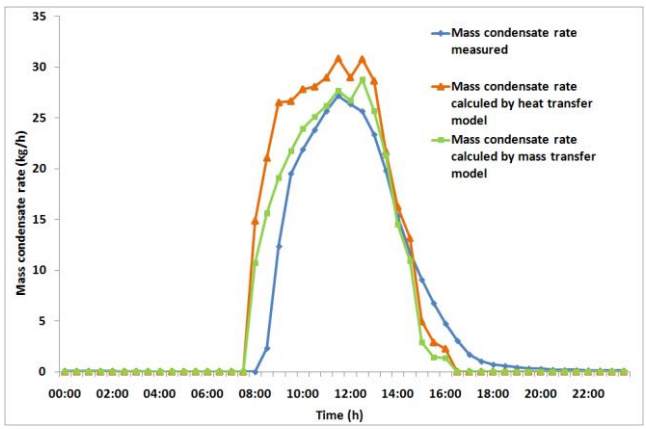

Figure 2 Comparison of the diurnal measured and calculated mass condensate rate of condenser.

Figure 3 shows the variation of the measured and the predicted mass condensate rates together with the solar radiation. The data were depicted every half an hour. It can be seen that the solar radiation values were observed only during the interval from 08:00 to 18:00 and it was almost null during the night time. In general, it can be noted that the amount of the calculated and measured mass condensate rates went hand-in-hand with solar radiation.

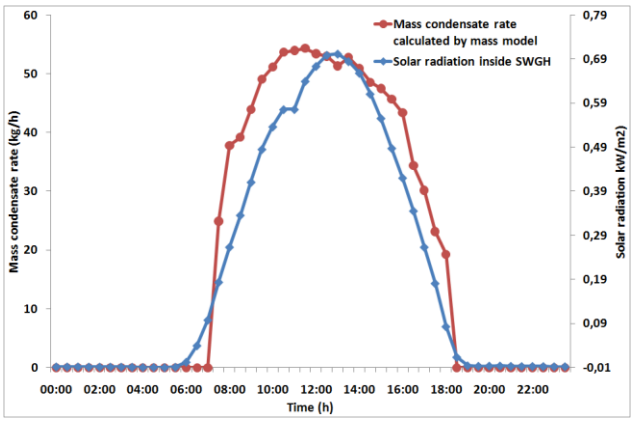

Figure 3 Comparison of the diurnal mass condensate rate and the solar radiation inside the SWGH.

The influence of the inlet relative humidity on fresh water produced by the condenser is shown in Figure 4. It can be seen that the simulation results by mass model give an increasing trend of the curve $\dot{m}_{c2} = f(RH)$. It is clear from the figure that as the relative humidity increases, the mass condensate rate is increased as well. Indeed, increasing the relative humidity of air entering the condenser leads to a large heat exchange. This heat exchange of latent heat is balanced by the activation of condensation which results in higher flows.

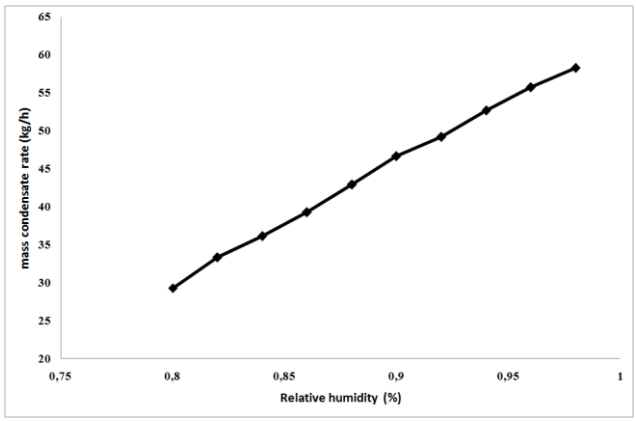

Figure 4 Influence of the relative humidity on fresh water produced by desalination in seawater greenhouse at Al-Hail, Muscat, Oman.

Figure 5 shows the influence of the inlet dry bulb temperature of air on fresh water produced by the condenser. For a variation of air temperature falling from 34 to 50 °C, the results of simulation by mass model of the function of the condenser at atmospheric pressure shows that the flow of condensate is strongly associated with ambient air conditions. It is evident from the figure that as the dry bulb temperature of air increases, as the productivity of fresh water is increased. For air temperatures rising and humidity constant, we note that the achievement of saturation conditions remains the major obstacle to condensation. Therefore, we can run through the condenser air recycling in the greenhouse to reach the saturation conditions.

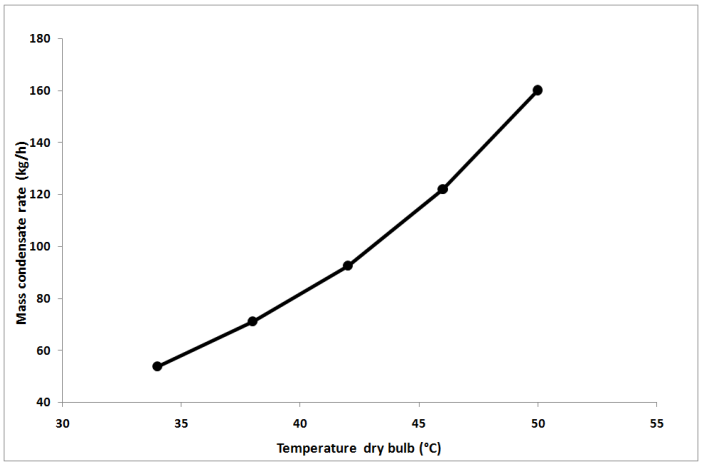

Figure 5 Influence of the dry bulb temperature on the fresh water produced by desalination in seawater greenhouse at Al-Hail, Muscat, Oman.

The influence of the inlet seawater temperature on the fresh water produced by the condenser is shown in Figure 6. For condensation conditions dictated by the vapor pressure of the gas phase, any increase of (T_{swin}) results in the displacement of temperature differences to the unfavorable areas. This shows that decreasing linear tendency is observed when the inlet temperature of the cold current (T_{swin}) increases. The outlet temperature of seawater consequently increases in a linear fashion with a negative impact on the mass flow of condensate. An average temperature of 25°C seems to flow trampling the optimal performance of the process.

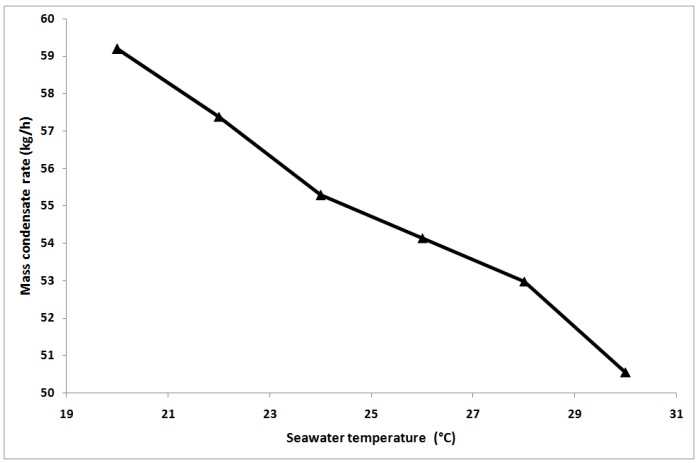

Figure 6 Influence of the seawater temperature on the fresh water produced by desalination in seawater greenhouse at Al-Hail, Muscat, Oman.

Figure 7 shows the influence of the inlet humid air mass flow on fresh water produced by the condenser in the seawater greenhouse at Al-Hail, Muscat, Oman. Any increase in mass flow leads to an increase in the amount of heat the incoming air and therefore the temperature of incoming air, thus increasing the flow of condensate. Indeed, any increase of speed of the humid air flow is spotted by an intensification of heat exchange given the impact of turbulence on the one hand reduces the film thickness of condensate and promoting the transfer of vapor to the tube wall on the other.

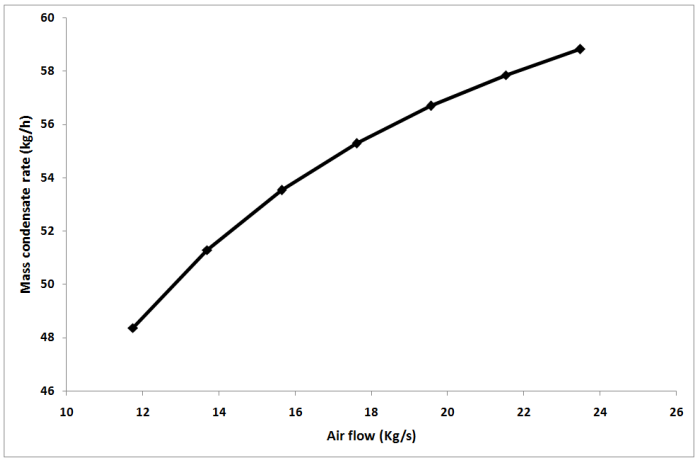

Figure 7 Influence of the air flow on the fresh water produced by desalination in seawater greenhouse at Al-Hail, Muscat, Oman.

The influence of the inlet seawater mass flow on the fresh water produced by the condenser is illustrated in Figure 8. It can be noted that the simulation results by mass model give a decreasing trend of the curve $\dot{m}_{c2} = f(\dot{m}_{sw})$. It is clear from the figure that as the inlet seawater mass flow decreases, the mass condensate rate is decreased. This situation offers better conditions for condensation and consequently the performance of the greenhouse.

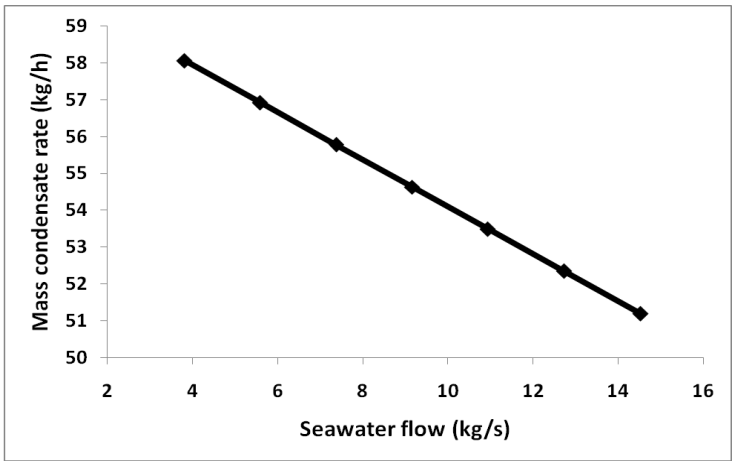

Figure 8 Influence of the seawater flow on the fresh water produced by desalination in seawater greenhouse at Al-Hail, Muscat, Oman.

CONCLUSIONS

This paper discussed the modeling of the heat and mass exchange in the condenser of a seawater greenhouse (SWGH) at Al Hail in Muscat, Oman. In this work, two theoretical models were developed in order to describe the process of condensation by using model of heat and mass transfer equations. A comparison was made between the mass condensate rates values calculated by the two models. The predicted values were also compared with that of the measured values. The trend of the predicted mass condensate rates calculated by mass model in this work was found much closer to the measured mass condensate rates. The results indicated that the comparison was more consistent with the mass model used in this work. Thus, we discussed the simulation of the influence of the operating parameters such as the dry bulb temperature of humid air, the relative humidity of air, the seawater temperature, the humid air flow and the seawater flow on fresh water produced by the condenser of seawater greenhouse. The results showed the influence of these parameters on the flow of condensate. It can be noted that the condensate flow rate increases with relative humidity of air, temperature of air entering and air flow. But the temperature of seawater and the flow of seawater affect negatively the flow of condensate.

NOMENCLATURE

A	heat transfer area, m^2
C_p	specific heat, J/kg K
C_s	mass humid heat, J/kg.K
D	diameter, m
D	mass diffusivities, m^2/s
f	friction factor
g	gravitational constant, m^2/s
h	heat transfer coefficient, W/m^2 °C
H	absolute humidity, kg water vapor/kg dry air
H	enthalpy, J/kg
h_{fg}	latent heat of vaporization, J/kg
h^*_{fg}	modified latent heat of vaporization, J/kg
h^0_{fg}	latent heat of vaporization at T=0°C, J/kg
k	thermal conductivity, W/m °C
L	length, m
Le	Lewis number
m	mass, kg
$\dot{m}$	mass flux, kg/s
N	number
Nu	Nusselt number
Pr	Prandtl number
Q	heat flux, W
RH	relative humidity, %
Sc	Schmidt number
St	Stanton number
T	temperature, °C

u velocity, m/s
y wall coordinate, m
x streamwise coordinate
X noncondensable gas mass fraction, kg noncondensable gas /kg total air
α Thermal diffusivities, m^2/s
δ film thickness, m
ρ density, kg/m^3
τ shear stress, N/m^2
Γ mass flux rate per unit length, kg/s m
μ Dynamic viscosity, kg/m s
ν kinematic viscosity, m^2/s

REFERENCES

Çengel, **Y.A. (2003).** Heat Transfer: a practical approach, *McGrRAW-HILL*, Vol. 2, pp. 532-552.

Davies, P.A., Paton, **C. (2005).** The Seawater Greenhouse in the United Arab Emirates: thermal modeling and evaluation of design options, *Desalination*, Vol. 173, pp. 103-111.

Davies, P.A., Turner, K., Paton, **C. (2004).** Potential of the seawater greenhouse in Middle Eastern Climates, *International Engineering Conference (IEC)*, Mutah, JORDAN.

Dawoud, B., Zurigat, Y.H., Klitzing, B., Aldoss, T., Theodoridis, **G. (2006).** On the possible techniques to cool the condenser of seawter greenhouse, *Desalination*, Vol. 195, pp. 119-140.

Douani, M., Tahri, T., Abdul-Wahab, S.A., Bettahar, A., Al-Hinai, H., Al-Mulla, Y. (2011). Modeling heat exchange in the condenser of a seawater greenhouse in Oman, *Chemical Engineering Communications*, Vol. 198, pp. 1-15.

Goosen, M.F.A., Sablani, S.S., Al-Hinai, H., Paton, C., Shayya, W.H. (2011). Humidification-Dehumidification Desalination: Seawater Greenhouse Development, *IDA World Congress on Desalination and Water Reuse*, Manama, Bahrain.

Maheshwari, N. K., Saha, D., Sinha, R. K., Aritomiet, **M. (2004).** Investigation on condensation in presence of a noncondensable gas for a wide range of Reynolds number, *Nucl. Eng. Des*. Vol. 227, pp. 219-238.

Mahmoudi, H., Spahis, N., Abdul-Wahab, S.A., Sablani, S.S., Goosen, **M.F.A. (2010).** Improving the performance of a Seawater Greenhouse desalination system by assessment of simulation models for different condensers, *Renewable and Sustainable Energy Reviews*, Vol. 14, pp. 2182-2188.

Nusselt, W. (1916). Die oberflachen Kondensation des Wasserdampes, *Z. Ver. Deut. Ing*. Vol. 60, pp. 541-546.

Paton, C., Davies, P.A. (2006). The seawater greenhouse cooling, fresh water and fresh produce from seawater, *The 2nd International Conference on Water Resources in Arid Environments*, Riyadh, KSA.

Perret, J.S., Al-Ismaili, A.M., Sablani, **S.S. (2005).** Development of humidification-dehumidification system in a quonset greenhouse for sustainable crop production in arid regions, *Biosystems Engineering*, Vol. 91, pp. 349-359.

Rohsenow, **W.M. (1952).** A Method of Correlating Heat Transfer Data for Surface Boiling of Liquid, *ASME Transactions*, Vol. 74, pp. 969-975.

Sacadura, **J.F. (1982).** Initition aux transferts thermiques, *Edit. Techniques et documentation*.

Seungmin, O., Revankar, **S.T. (2006).** Experimental and theoretical investigation of film condensation with noncondensable gas, *Int. J. HEAT and MASS TRANSFER*, Vol. 49, pp. 2523-2534.

Sherwood, T.K., Comings, **E.W. (1932).** An experimental study of the wet bulb hygrometer, *Trans. Am. Inst. Chem. Eng*., Vol. 28, pp. 88.

Tahri, T., Abdul-Wahab, S.A., Douani, M., Bettahar, A., Al-Hinai, H., Al-Mulla, Y. (2009). Simulation of the condenser of the seawater greenhouse. Part I: Theoretical development, *Journal of Thermal Analysis and Calorimetry*. Vol. 96, pp. 43-47.